ORIGINAL ARTICLE

Molecular Plant Pathology | WILEY

Synergistic interaction between the type III secretion system of the endophytic bacterium *Pantoea agglomerans* DAPP-PG 734 and the virulence of the causal agent of olive knot *Pseudomonas savastanoi* pv. *savastanoi* DAPP-PG 722

Chiaraluce Moretti[1] | Fabio Rezzonico[2] | Benedetta Orfei[1] | Chiara Cortese[1] | Alba Moreno-Pérez[3,4] | Harrold A. van den Burg[5] | Andrea Onofri[1] | Giuseppe Firrao[6] | Cayo Ramos[3,4] | Theo H. M. Smits[2] | Roberto Buonaurio[1]

[1]Dipartimento di Scienze Agrarie, Alimentari e Ambientali, Università degli Studi di Perugia, Perugia, Italy

[2]Environmental Genomics and Systems Biology Research Group, Institute of Natural Resource Sciences, Zurich University of Applied Sciences ZHAW, Wädenswil, Switzerland

[3]Área de Genética, Facultad de Ciencias, Universidad de Málaga, Málaga, Spain

[4]Instituto de Hortofruticultura Subtropical y Mediterránea "La Mayora", Universidad de Málaga-Consejo Superior de Investigaciones Científicas, Málaga, Spain

[5]Molecular Plant Pathology, Swammerdam Institute for Life Sciences, University of Amsterdam, Amsterdam, Netherlands

[6]Dipartimento di Scienze Agroalimentati Ambientali e Animali, Università degli Studi di Udine, Udine, Italy

Correspondence
Chiaraluce Moretti, Dipartimento di Scienze Agrarie, Alimentari e Ambientali, Università degli Studi di Perugia, Borgo XX Giugno 74, 06121 Perugia, Italy.
Email: chiaraluce.moretti@unipg.it

Abstract

The endophytic bacterium *Pantoea agglomerans* DAPP-PG 734 was previously isolated from olive knots caused by infection with *Pseudomonas savastanoi* pv. *savastanoi* DAPP-PG 722. Whole-genome analysis of this *P. agglomerans* strain revealed the presence of a *Hypersensitive response and pathogenicity* (*Hrp*) type III secretion system (T3SS). To assess the role of the *P. agglomerans* T3SS in the interaction with *P. savastanoi* pv. *savastanoi*, we generated independent knockout mutants in three *Hrp* genes of the *P. agglomerans* DAPP-PG 734 T3SS (*hrpJ*, *hrpN*, and *hrpY*). In contrast to the wildtype control, all three mutants failed to cause a hypersensitive response when infiltrated in tobacco leaves, suggesting that *P. agglomerans* T3SS is functional and injects effector proteins in plant cells. In contrast to *P. savastanoi* pv. *savastanoi* DAPP-PG 722, the wildtype strain *P. agglomerans* DAPP-PG 734 and its *Hrp* T3SS mutants did not cause olive knot disease in 1-year-old olive plants. Coinoculation of *P. savastanoi* pv. *savastanoi* with *P. agglomerans* wildtype strains did not significantly change the knot size, while the DAPP-PG 734 *hrpY* mutant induced a significant decrease in knot size, which could be complemented by providing *hrpY* on a plasmid. By epifluorescence microscopy and confocal laser scanning microscopy, we found that the localization patterns in knots were nonoverlapping for *P. savastanoi* pv. *savastanoi* and *P. agglomerans* when coinoculated. Our results suggest that suppression of olive plant defences mediated by the *Hrp* T3SS of *P. agglomerans* DAPP-PG 734 positively impacts the virulence of *P. savastanoi* pv. *savastanoi* DAPP-PG 722.

KEYWORDS
endophyte, hypersensitive reaction, mutant, olive knot community, *Pantoea agglomerans*, *Pseudomonas savastanoi* pv. *savastanoi*, *Pseudomonas syringae* complex, T3SS

1 | INTRODUCTION

Olive knot disease, caused by *Pseudomonas savastanoi* pv. *savastanoi*, is one of the most important diseases of olive trees (*Olea europaea*) in many olive-producing areas, where it can provoke severe reductions in vegetative growth and yield (Quesada et al., 2012; Schroth et al., 1973). There is increasing interest on olive knot disease as a molecular model of a woody plant disease (Caballo-Ponce et al., 2017a, 2017b; Moreno-Pérez et al., 2020; Moretti et al., 2019; Ramos et al., 2012) and it is also considered a model system for studying the role of interspecies bacterial communities in plant disease development (Buonaurio et al., 2015; Hosni et al., 2011; Passos da Silva et al., 2014). A metagenomics study performed on olive knots isolated from different olive cultivars revealed that a large number of endophytic bacteria was present inside the knots and, among these, the most representative belong to the genera *Pantoea*, *Erwinia*, and *Pectobacterium* (Passos da Silva et al., 2014). This raised the question about the role of interspecies bacterial communities in plant diseases (Buonaurio et al., 2015). Among the complex olive-knot microbiome, the by-themselves nonpathogenic bacterial species *Erwinia toletana*, *Pantoea agglomerans*, and *Erwinia oleae*, which were frequently isolated from olive knots, cooperate with *P. savastanoi* pv. *savastanoi* in that they positively modulate the disease severity (Buonaurio et al., 2015). For example, coinoculations of *E. toletana* with *P. savastanoi* pv. *savastanoi* resulted in an increased size of the knots and in an enhanced bacterial colonization compared to single inoculations of the pathogen alone (Buonaurio et al., 2015; Hosni et al., 2011).

The genus *Pantoea* comprises many versatile species isolated from several aquatic and terrestrial environments both as free-living organisms or in association with insects, animals, humans, and plants (Walterson & Stavrinides, 2015). Several members of the *Pantoea* genus have been recognized as common plant epiphytes and endophytes (Kobayashi & Palumbo, 2000; Lindow & Brandl, 2003), while others are true plant pathogens causing galls, wilting, soft rot, and/ or necrosis in a variety of agriculturally relevant plants (Walterson & Stavrinides, 2015). Plant pathogenicity and virulence of *Pantoea* spp. is in some cases influenced by a suite of factors that include the type III secretion system (T3SS), quorum-sensing (QS) regulation, exopolysaccharide (EPS) production, and indole-3-acetic acid (IAA) and cytokinin biosynthesis (Chalupowicz et al., 2008, 2009; Panijel et al., 2013; Roper, 2011; Walterson & Stavrinides, 2015). Gall formation by *Pantoea agglomerans* pv. *gypsophilae*, and *P. agglomerans* pv. *betae* on gypsophila and beet, respectively, is dependent on the acquisition of a plasmid containing a functional *Hrp* gene cluster encoding the type III secretion system (T3SS) (Barash & Manulis-Sasson, 2009; Kirzinger et al., 2015; Manulis et al., 1991a; Weinthal et al., 2007) and a gene cluster for IAA and cytokinin biosynthesis (Barash & Manulis-Sasson, 2009; Manulis & Barash, 2003; Manulis et al., 1991b).

P. agglomerans isolates that produce comparable high levels of IAA in vitro compared to those produced by *P. savastanoi* pv. *savastanoi* are frequently obtained from olive knots (Hosni, 2010). When inoculated on tobacco leaves, these *P. agglomerans* strains are able to elicit a hypersensitive response (HR), indicating that they contain a functional T3SS that secretes effector proteins (Moretti et al., 2014). However, single inoculation of these *P. agglomerans* strains on olive plants does not cause olive knot disease.

Among the *P. agglomerans* strains isolated from knots, we have primarily focused on *P. agglomerans* DAPP-PG 734, which forms a stable interspecies community with *P. savastanoi* pv. *savastanoi* DAPP-PG 722 (Buonaurio et al., 2015; Hosni et al., 2011) and whose genome sequence has been reported (Moretti et al., 2014). In the same fashion as *E. toletana* DAPP-PG 735 (Caballo-Ponce et al., 2018; Passos da Silva et al., 2014), *P. agglomerans* DAPP-PG 734 communicates with *P. savastanoi* pv. *savastanoi* DAPP-PG 722 through a QS system mediated by *N*-acyl-homoserine lactones (AHLs) (Buonaurio et al., 2015; Hosni et al., 2011). When coinoculated in olive plants with a mutant of the pathogen unable to synthesize AHLs, *P. agglomerans* DAPP-PG 734 stimulates growth of *P. savastanoi* pv. *savastanoi* DAPP-PG 722 and moderately increases olive knot disease severity (Hosni, 2010). This cooperation was suggested to be due to growth stimulation and phytohormone production by the endophyte, as well as by the interspecies interactions mediated by the diffusible AHL signal molecules (Buonaurio et al., 2015; Hosni et al., 2011).

The aim of this study was to investigate the role of *P. agglomerans* T3SS in the interspecies interaction that takes place between *P. savastanoi* pv. *savastanoi* DAPP-PG 722 and *P. agglomerans* DAPP-PG 734 in olive knots. For this purpose, we performed a bioinformatics analysis of the *P. agglomerans* DAPP-PG 734 genome (Moretti et al., 2014) directed to its T3SS and effectors. The phylogenetic relationship between 119 *P. agglomerans* strains, including *P. agglomerans* DAPP-PG 734, and six closely related *Pantoea* species was investigated by core genome phylogenomic analysis and related to the T3SS content of these genomes. Because *P. agglomerans* DAPP-PG 734 seems to have a functional *Hrp*-encoded T3SS, its role in olive knot disease was studied by constructing knockout mutants of the T3SS genes *hrpJ*, *hrpN*, and *hrpY*. Lastly, the localization of *P. agglomerans* DAPP-PG 734 and *P. savastanoi* pv. *savastanoi* DAPP-PG 722 within the knots was investigated by using epifluorescence stereoscopic microscopy and confocal laser scanning microscopy (CLSM).

2 | RESULTS

2.1 | *P. agglomerans* DAPP-PG 734 phylogenomic position

To verify the phylogenomic position, a total of 119 genomes of *P. agglomerans* and related *Pantoea* spp. were compared. Phylogenomic analysis (Figure 1) using the core genome of these strains revealed that several genomes present in the NCBI database were incorrectly assigned to certain species, while most sequences labelled as *Pantoea* sp. could be included in known species. Using average nucleotide identity (ANI) in EDGAR, assignment at species level was examined (Figure 1). Based on the core tree, it was confirmed that
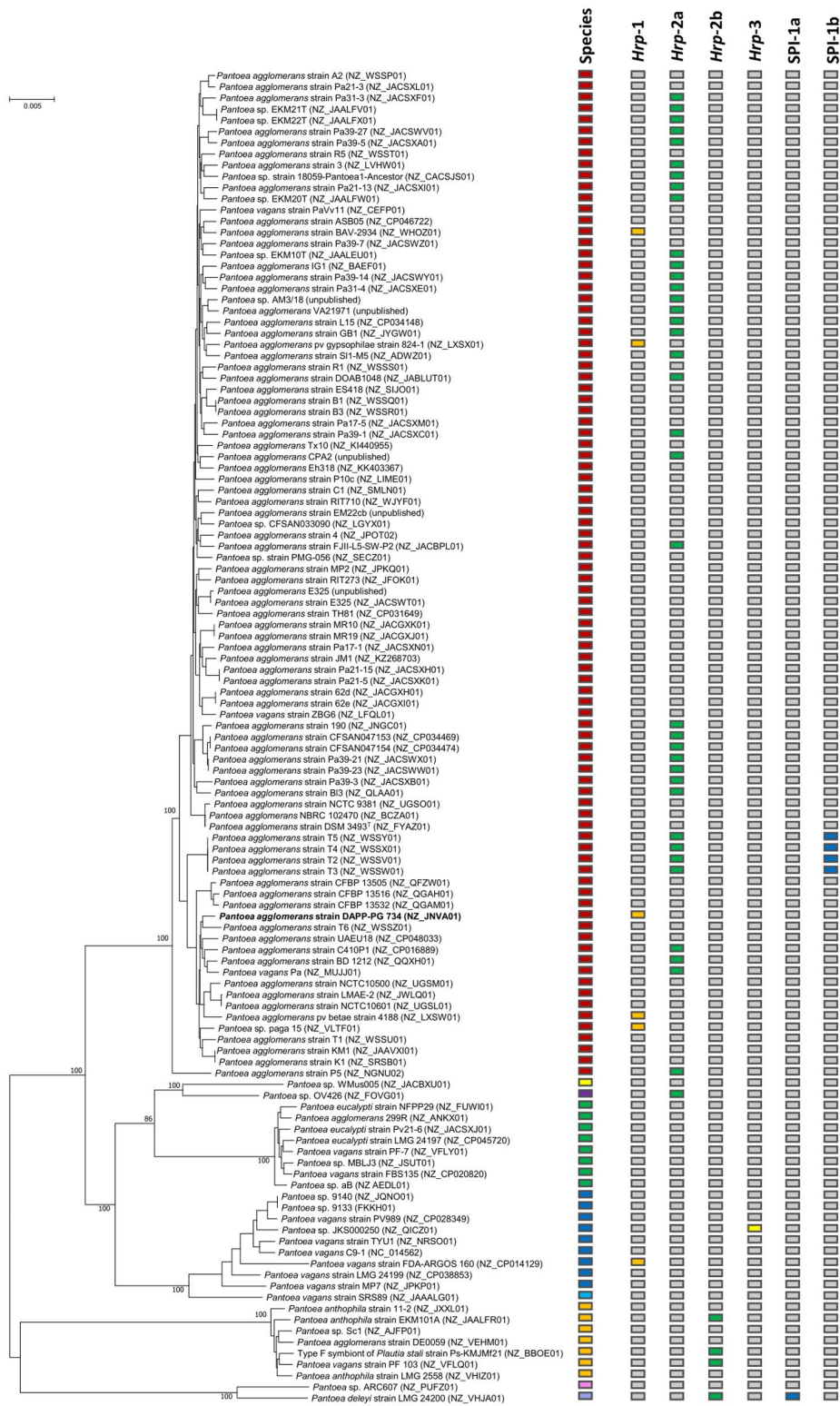
FIGURE 1 Phylogenomic core genome tree of the *Pantoea* spp. analysed in this study constructed using FastTree in EDGAR and the presence of *Hrp* type III secretion systems in individual strains, as indicated by different coloured boxes (*Hrp*-1, orange; *Hrp*-2, green; *Hrp*-3, blue). Grey boxes indicate absence in the respective strain. Species delineation based on ANI values >95% are indicated using coloured boxes for each species

P. agglomerans DAPP-PG 734 was a typical member of the species *P. agglomerans*.

2.2 | Detailed analysis of the T3SS of *P. agglomerans* and related species

To analyse the T3SS of *P. agglomerans* and related species, a comparison of the *P. agglomerans* DAPP-PG 734 genome with those of other *P. agglomerans* and *Pantoea* spp. strains was carried out. It revealed that DAPP-PG 734 harbours at least three plasmids, which have relatives in other *Pantoea* spp. (Smits et al., 2011). However, the assembly of the plasmids is not complete, but the contigs that were identified as belonging to plasmids based on orthology to known complete plasmids show that there is large variance in the gene content when comparing the same plasmid in different strains (de Maayer et al., 2012).

In silico analysis identified a 94-kb contig (GenBank acc. no. NZ_JNVA01000006) in the genome of *P. agglomerans* DAPP-PG 734 that contained (a) the entire *Hrp*-1 T3SS gene cluster; (b) a *repA* gene encoding the enzyme essential for plasmid replication; (c) a complete conjugal transfer system; and (d) several plasmid maintenance proteins. These features indicated that the T3SS in *P. agglomerans* DAPP-PG 734 is potentially located on a plasmid. However, the plasmid could not be proven circular by read mapping.

The *Hrp*-1 T3SS cluster in *P. agglomerans* DAPP-PG 734 (Figure 2) is highly similar in its composition to the well-characterized *Hrp* T3SSs of the bacteria *Pantoea stewartii* subsp. *stewartii* DC283 (Frederick et al., 2001) and *Erwinia amylovora* CFBP 1430 (Oh et al., 2005; Smits et al., 2010), having a complete *Hrp* effectors and elicitors (HEE) region belonging to the T3SS category VI (Hu et al., 2017). Similar gene clusters were found in *P. agglomerans* BAV 2934 and in *Pantoea vagans* FDA-ARGOS 160. In the latter two strains, the *Hrp*-1 T3SS is potentially located on a plasmid as well. However, the *Hrp*-1 T3SS clusters of *P. agglomerans* pv. *gypsophila* 824-1, *P. agglomerans* pv. *betae* 4188, and a further strain, *P. agglomerans* paga 15, do not have the full HEE region (Figure 2).

The pan-genome analysis indicated the presence of different types of T3SSs in the genomes. Forty-two strains contained an *Hrp*-2 T3SS, in which the genes have a different order than in the *Hrp*-1 cluster (Kirzinger et al., 2015). Among them, four strains (*Pantoea deleyi* LMG 24200 and three *Pantoea anthophila* strains) contained the *dspA/E* and *dspF* genes as a second additional copy (*Hrp*-2b). All other isolates also contained the type III helper gene *hopP1* in close vicinity to the cluster (*Hrp*-2a). *P. vagans* JKS000250 contained a third *Hrp* T3SS (*Hrp*-3) in which the absence of *hrpXY* was the most peculiar feature (Figure 2). *P. deleyi* LMG 24200 contains additionally an SPI-1a T3SS highly similar to the SPI T3SSs of *P. stewartii* subsp. *stewartii* DC283 (Correa et al., 2012) or *E. amylovora* CFBP 1430 (Kamber et al., 2012; Smits et al., 2010), while the SPI-1b T3SS clusters of four wheat isolates of *P. agglomerans* were different in the putative effector region of this system (Figure 2). The four wheat isolates also contain a full *Hrp*-2a.

## 2.3 | Comparison of Hrp T3SSs in *Pantoea* spp. and related organisms

To examine the origin of the *Hrp*-1 of DAPP-PG 734, we compared the different Hrp T3SSs using a multilocus sequence typing (MLST) approach in which the protein sequences of HrcC, HrcN, HrcU, and HrcV were concatenated and used for a cluster analysis. The dendrogram in Figure 3 reveals that the *Hrp*-1 T3SS of *P. agglomerans* DAPP-PG 734 was most closely related to that of *P. agglomerans* BAV 2934 and *P. vagans* FDA-ARGOS 160, but also to the *Hrp* T3SS of *Erwinia mallotivora* BT-MARDI. The *Hrp*-1 T3SS of *P. agglomerans* pv. *gypsophila* 824-1, *P. agglomerans* pv. *betae* 4188, and *P. agglomerans* paga 15 clustered more distantly, and closer to the *Hrp* T3SS of *P. stewartii* subsp. *stewartii* DC283 (Frederick et al., 2001). The Hrp T3SS of *E. amylovora* CFBP 1430 and related plant-pathogenic *Erwinia* spp. (Kamber et al., 2012) were more distantly positioned. Thus, a clear answer to the origin of the *Hrp*-1 cluster cannot be derived, as there is evidence that all closely related T3SS are of foreign origin (Kirzinger et al., 2015).

## 2.4 | Effector genes for the T3SSs in *Pantoea* spp.

Few T3SS effector genes were identified in the HEE region of the *Hrp*-1 T3SS of *P. agglomerans* DAPP-PG 734 and BAV 2934 and *P. vagans* FDA-ARGOS 160, which were not present within the HEE region of the plant pathogens *P. agglomerans* pv. *gypsophila* 824-1 and *P. agglomerans* pv. *betae* 4188 (Table 1). On the other hand, most T3SS effectors identified in the latter two strains (Nissan et al., 2018) did not have orthologs in the other genomes. This shows that the T3SS of *P. agglomerans* pv. *gypsophila* 824-1 and *P. agglomerans* pv. *betae* 4188 rely greatly on the pathogenic potential encoded on the respective plasmids (Barash & Manulis-Sasson, 2009), whereas the *Hrp* T3SSs in *P. agglomerans* strains DAPP-PG 734 and BAV 2934 and *P. vagans* FDA-ARGOS 160 have a more limited T3SS effector arsenal.

2.5 | Phenotypic characterization of *P. agglomerans* *Hrp*-1 mutants

We previously reported that *P. agglomerans* DAPP-PG 734 can induce an HR in tobacco plants (Moretti et al., 2014). To assess whether the here-identified *Hrp*-1 T3SS is required for HR induction, we generated three independent mutants in different genes of the *Hrp*-1 cluster. The *hrpJ*, *hrpN*, and *hrpY* genes were chosen on the basis of the function of the encoded proteins in the T3SS as structural protein, effector, and regulatory protein, respectively. In particular, it was demonstrated earlier that regulation of the PSI-1 T3SS involves the HrpX/HrpY two-component regulatory system (Mor et al., 2001; Merighi et al., 2003, 2006). HrpY acts downstream in the activation of *hrpS*, which subsequently regulates the *hrpL* gene,
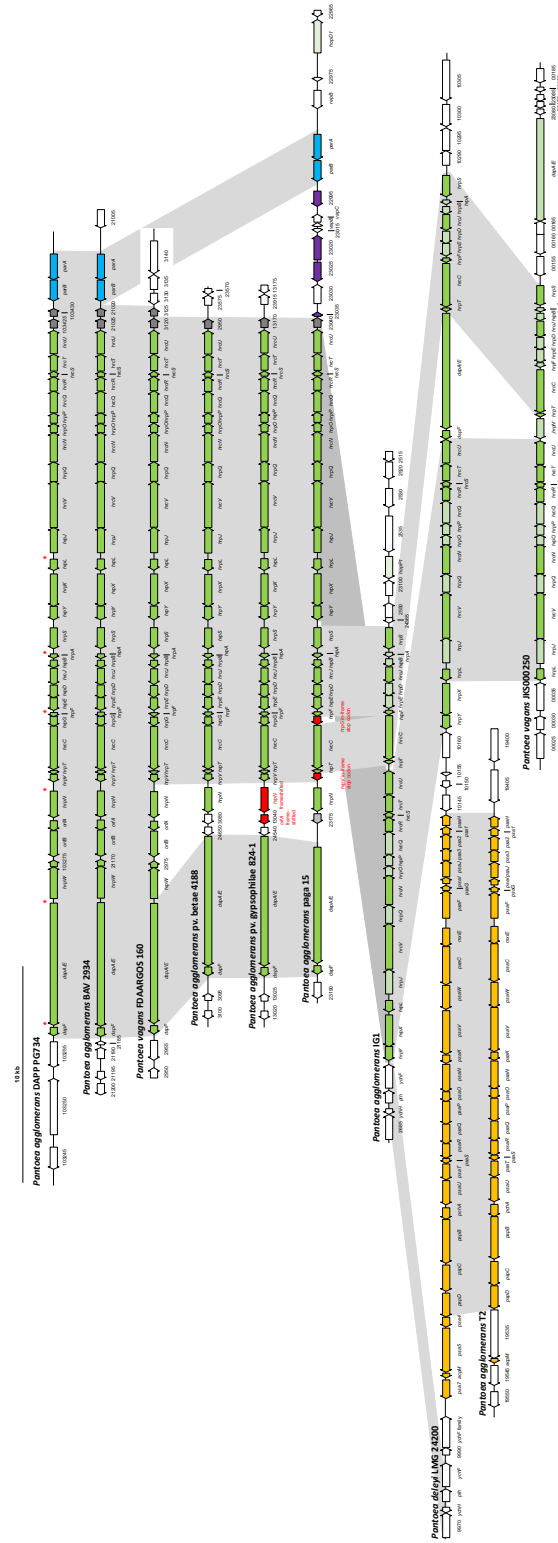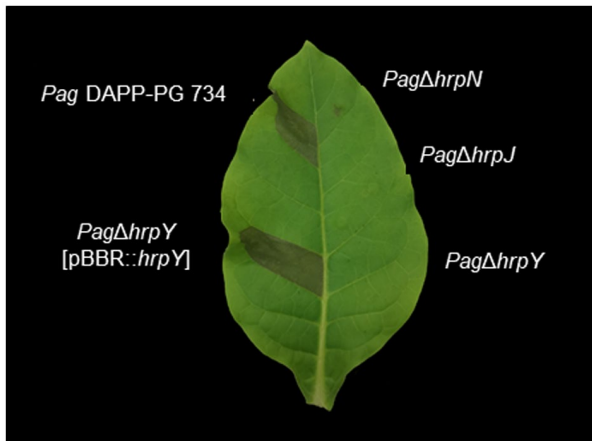
FIGURE 2 Hrp clusters in *Pantoea* spp. All *Hrp*-1 and representative species for other *Hrp* type III secretion systems (T3SSs) are shown. Green arrows represent *Hrp*-1 structural and effector genes, red arrows are frameshifted genes. In *Hrp*-2 and *Hrp*-3 T3SS, light green arrows indicate lower sequence identity to the genes in *Hrp*-1. The SPI-1 and SPI-2 clusters are given with orange arrows. Additional colours: light blue, plasmid-related genes; purple, transposon-related genes; grey, conserved genes; white, unrelated genes. The red asterisks at the line for *Pantoea agglomerans* DAPP-PG 734 indicate the presence of *Hrp* boxes (see Table S1)
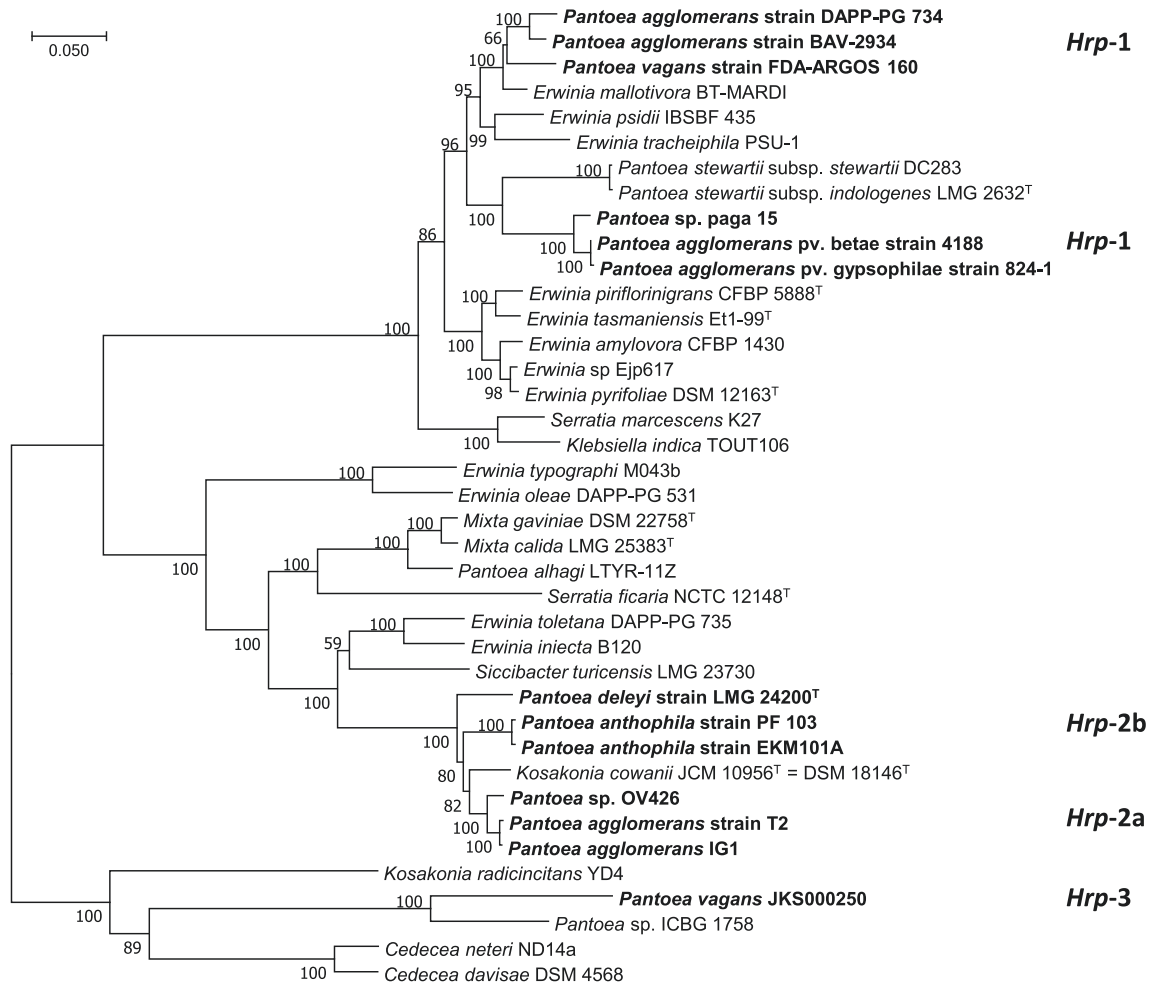
FIGURE 3 Unrooted neighbour-joining tree of concatenated HrcC-HrcN-HrcU-HrcV protein sequences of *Hrp* type III secretion systems (T3SSs). Bootstrap values (1,000 repeats) are indicated at the branches. The *Hrp* T3SS systems discussed in this paper are indicated in bold

TABLE 1 Effectors in the genomes of *Pantoea* spp. containing the *Hrp*-1 T3SS

Effector	Reference sequence (locus tag)	P. agglomerans DAPP-PG 734	P. agglomerans BAV-2934	P. vagans FDA-ARGOS 160	P. agglomerans pv. betae 4188	P. agglomerans pv. gypsophilae 824-1	P. agglomerans paga 15	P. agglomerans IG1 (HRP-2a)
hrpN	GS10_RS0103295	+	+	+	+	−	+	−
orfB	GS10_RS0103285	+	+	+	−	−	−	−
hrpW	GS10_RS0103270	+	+	+	−	−	−	−
dspA/E	GS10_RS0103265	+	+	+	+	+	+	−
hopQ1	A7P61_RS08055	−	−	−	+	−	+	−
hopD1	A7P62_RS10595	−	−	−	−	+	+	−
hopAY1	A7P61_RS11580	−	−	−	+	+	−	−
hopAF1	A7P62_RS00640	−	−	−	+	+	−	−
hopAK1	A7P62_RS00650	−	−	−	+	+	−	−
hopV1	A7P62_RS00655	−	−	−	+	+	−	−
xopE2	A7P62_RS10630	−	−	−	+	+	−	−
hsvG	A7P62_RS10725	−	−	−	+	+	−	−
hsvB	A7P62_RS10575	−	−	−	+	+	−	−
pthG	A7P62_RS18080	−	−	−	+	+	−	−
pseB	A7P61_RS24765	−	−	−	−	+	+	−

FIGURE 4 Hypersensitive response on tobacco leaf 24 hr after inoculation with *Pantoea agglomerans* DAPP-PG 734 (wild type) or the mutants *PagΔhrpJ*, *PagΔhrpN*, *PagΔhrpY*, and the complemented strain *PagΔhrpY*[pBBR::*hrpY*]

and HrpL induces expression of genes containing a "*hrp* box" regulatory element in their promoter.

The three mutants and the wildtype strain *P. agglomerans* DAPP-PG 734 were tested for induction of an HR in tobacco. In contrast to the wildtype strain, the mutants failed to induce an HR in tobacco (Figure 4), indicating that the *Hrp*-1 T3SS and the HrpN protein are essential for this response.

To determine whether the *P. agglomerans* mutants are impaired in other phenotypic traits important for their endophytic lifestyles, several phenotypic features were tested (Text S1). Production of IAA was slightly reduced in the mutants as compared to the wildtype strain (Figure S1). No differences were observed with respect to the wild type in proteolytic and antibacterial activities against *P. savastanoi* pv. *savastanoi* DAPP-PG 722 and *Escherichia coli* in the production of siderophore, EPS, and AHL, or in swimming and swarming motility (Figure S2 and Table S2), indicating that the above-listed features are regulated independently of Hrp regulators.

2.6 | Influence of the *Hrp*-1 T3SS on the interaction between *P. savastanoi* pv. *savastanoi* DAPP-PG 722 and *P. agglomerans* DAPP-PG 734

To examine whether the interaction between *P. savastanoi* pv. *savastanoi* DAPP-PG 722 and *P. agglomerans* DAPP-PG 734 in olive knots is influenced by *P. agglomerans* Hrp-1 T3SS, the *P. agglomerans* mutants were coinoculated with the pathogen *P. savastanoi* pv. *savastanoi* DAPP-PG 722 on stems of 1-year-old wounded olive plants. Comparison of the coinoculation with both wildtype strains to the coinoculation with the *P. agglomerans* DAPP-PG 734 mutants showed a significant reduction in the knot volume induced by the *PagΔhrpY* mutant (Figure 5a). In olive plants inoculated with wildtype *P. agglomerans* DAPP-PG 734 or its *Hrp* mutants alone no disease symptoms, expressed as knot volume, were observed. Therefore, these "all-zero" treatments were not included in the analyses, so as not to hinder the basic assumptions for linear model fitting (Onofri et al., 2010).

Furthermore, *P. savastanoi* pv. *savastanoi* DAPP-PG 722 showed reduced proliferation in olive knots when it was coinoculated with *P. agglomerans* DAPP-PG 734 in olive plants, with respect to when it was inoculated alone. On the other hand, the population dynamic of *P. savastanoi* pv. *savastanoi*, measured as the number of bacterial cells per inoculation site, was similar to that observed when this pathogen was coinoculated with the *P. agglomerans* mutants, with respect to when it was inoculated alone (Figure 5b).

The bacterial growth of *P. agglomerans* DAPP-PG 734 and its *Hrp* mutants inoculated alone in olive plants slightly increased from 0 to 21 days postinoculation (dpi) and then declined (Figure 5b). This first increase in the bacterial growth, measured as the number of bacterial cells per inoculation site, was slightly but significantly attenuated when the mutant strains *PagΔhrpN* or *PagΔhrpY* were coinoculated with *P. savastanoi* pv. *savastanoi* DAPP-PG 722 (Figure 5b). However, the presence of *P. savastanoi* pv. *savastanoi* DAPP-PG 722 strongly increased the growth of the wildtype *P. agglomerans* DAPP-PG 734 and its *Hrp* mutants (Figure 5b). In addition, the growth of the mutants *PagΔhrpN* and *PagΔhrpY* was further enhanced by the presence of the coinoculated *P. savastanoi* pv. *savastanoi* with respect to the *P. agglomerans* DAPP-PG 734 wild type (Figure 5b). Based on these findings, it is highly likely that the bacterial endophyte *P. agglomerans* DAPP-PG 734 and *P. savastanoi* pv. *savastanoi* DAPP-PG 722 form a stable consortium in the knots and that this interaction is influenced by the *Hrp*-1 T3SS of *P. agglomerans* DAPP-PG 734.

2.7 | Complementation of the *PagΔhrpY* mutant

To assess whether the inability of the *PagΔhrpY* mutant to induce an HR and the formation of full-size knots in coinoculation experiment with *P. savastanoi* pv. *savastanoi* DAPP-PG 722 was due to the loss of the regulatory function of the protein encoded by the *hrpY* gene, complementation of the *PagΔhrpY* was performed using a plasmid expressing the *P. agglomerans* DAPP-PG 734 *hrpY* gene from the *E. coli lac* promoter (*PagΔhrpY*[pBBR::*hrpY*]). The ability of the complemented mutant strain to induce HR in tobacco leaf was restored (Figure 4). Knot overgrowth caused by coinoculation of *P. savastanoi* pv. *savastanoi* DAPP-PG 722 with the complemented strain *PagΔhrpY* (pBBR::*hrpY*) was not significantly different to that of *P. savastanoi* pv. *savastanoi* DAPP-PG 722 alone or coinoculated with wildtype *P. agglomerans* DAPP-PG 734 (Figure 5c). These results suggest that the commensal interaction established between *P. savastanoi* pv. *savastanoi* DAPP-PG 722 and *P. agglomerans* DAPP-PG 734 during knot formation in olive plants is dependent on the integrity of the *P. agglomerans* DAPP-PG 734 *Hrp*-1 T3SS.

2.8 | In planta localization of *P. savastanoi* pv. *savastanoi* DAPP-PG 722 and *P. agglomerans* DAPP-PG 734

To verify the position of *P. savastanoi* pv. *savastanoi* DAPP-PG 722 and *P. agglomerans* DAPP-PG 734 within the olive knots, fluorescently labelled cells of both strains were coinoculated in micropropagated

(a)

(b)

(c)
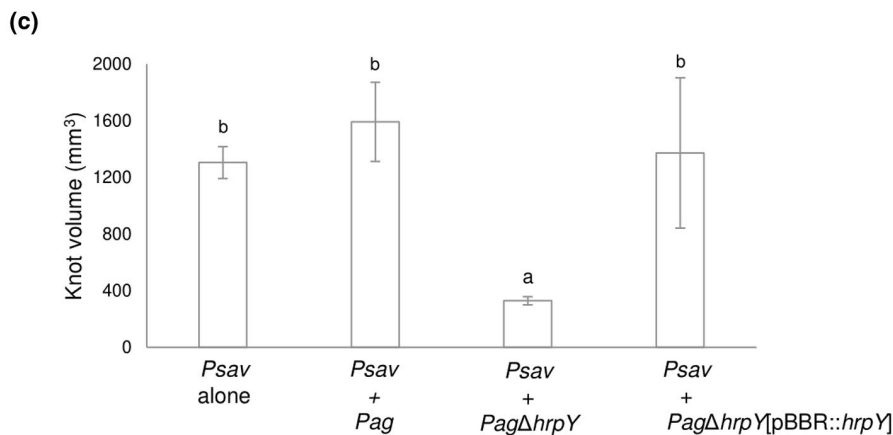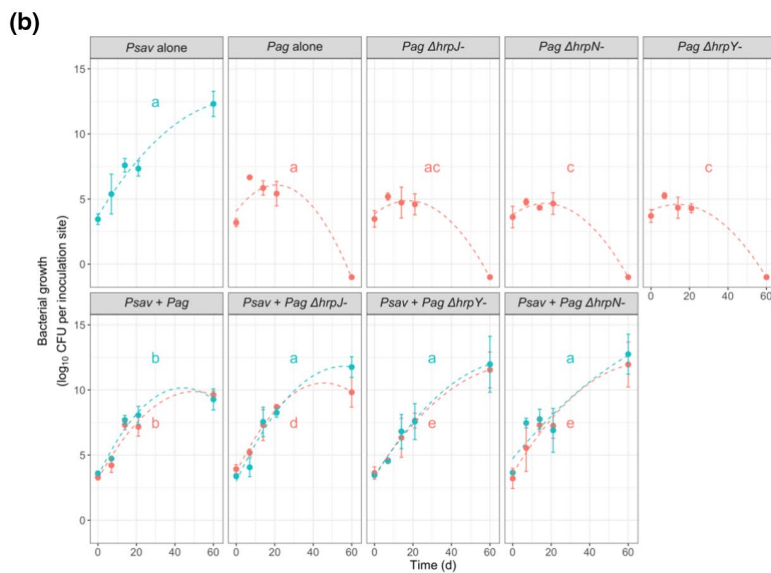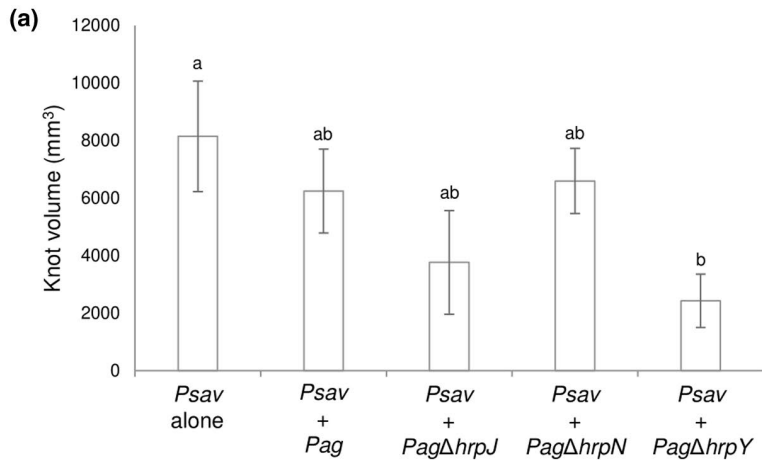
FIGURE 5 Effect of inoculation of *Pseudomonas savastanoi* pv. *savastanoi* DAPP-PG 722 (*Psav*) alone or in combination with *Pantoea agglomerans* (*Pag*) DAPP-PG 734 or its derivative mutants on knot formation (a, c) and in planta population dynamics (b). (a) Knot formation, expressed as stem overgrowth observed 60 days postinoculation (dpi), in 1-year-old olive (cv. Frantoio) stems inoculated with *Psav* alone or in combination with *Pag* or *PagΔhrpJ*, *PagΔhrpN*, *PagΔhrpY*. Each value is the mean ± *SE* of three replicates. Values with the same letter are not significantly different (*p* = 0.05) according to Duncan's multiple range test. (b) Growth of *Psav*, *Pag* or *PagΔhrpJ*, *PagΔhrpN*, *PagΔhrpY* alone or in combination in olive (cv. Frantoio) plants. The symbols indicate observed bacterial counts and the lines indicate the linear mixed model fit (blue, *Psav*; red, *Pag* and its mutants). For each bacterial species, different letters indicate a significant difference between growth curves. Vertical bars show standard errors. (c) Knot formation, expressed as stem overgrowth observed 60 dpi, in 1-year-old olive (cv. Frantoio) stems inoculated with *Psav* alone or in combination with *Pag* or *PagΔhrpY*, or complemented strain *PagΔhrpY*[pBBR::*hrpY*]. Each value is the mean ± *SE* of four replicates. Values with the same letter are not significantly different (*p* = 0.01) according to Duncan's multiple range test

olive plants. Epifluorescence microscopy revealed that RFP-labelled *P. agglomerans* (*Pag*-DRE) inoculated alone did not produce any disease symptoms and the low bacterial population reached by the strain only allowed detection of a red fluorescent spot at the inoculation site (Figure 6a). In contrast, when *P. agglomerans Pag*-DRE was coinoculated with GFP-labelled *P. savastanoi* pv. *savastanoi* (*Psav*-GFP), cells

of *Pag*-DRE were more abundant, and they became visible in the knot using epifluorescence microscopy. *P. agglomerans* was distributed in a nonhomogenous manner in knots and it was largely absent from areas with high bacterial density of *P. savastanoi* pv. *savastanoi* (Figure 6b). In contrast, *Psav*-GFP was uniformly distributed within the knot tissues both when inoculated alone (Figure 6a) or coinoculated with *Pag*-DRE
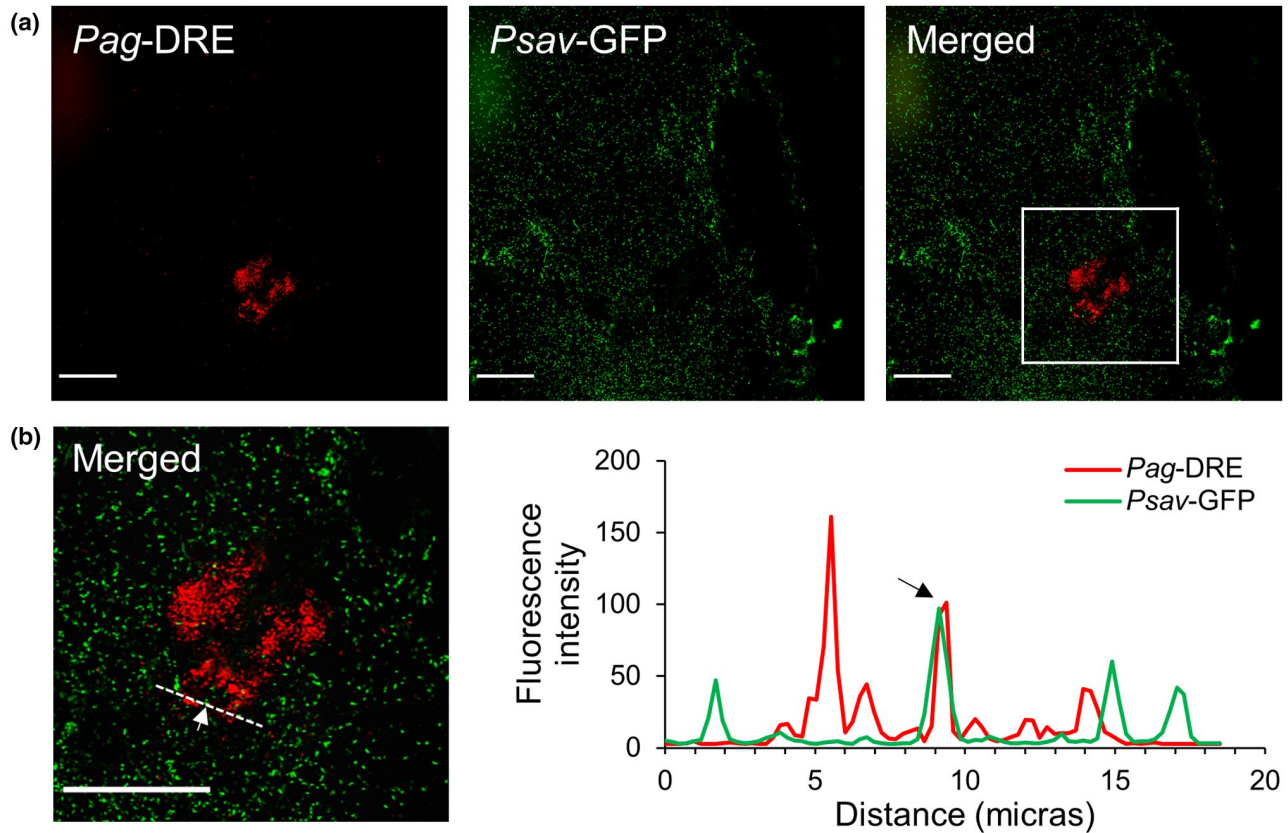
FIGURE 6 In planta localization of RFP-labelled *Pantoea agglomerans* DAPP-PG 734 (*Pag*-DRE) and GFP-labelled *Pseudomonas savastanoi* pv. *savastanoi* DAPP-PG 722 (*Psav*-GFP). (a, b) Epifluorescence microscopy of olive knots developed at 28 days postinoculation (dpi) in micropropagated olive plants. Knots induced by (a) independent inoculations of *Pag*-DRE and *Psav*-GFP or (b) by coinoculation of *Pag*-DRE and *Psav*-GFP. The diffused red colouration observed in (a) is due to the red autofluorescence of the plant. Images were acquired without filter (bright field), with a GFP filter or with an RFP filter. Merged, fusion of the GFP and RFP images. Bars = 2 mm. (c) Population dynamics of *Pag*-DRE in in vitro olive plants inoculated alone (*Psav*-GFP alone) or in combination with *Psav*-GFP (*Pag*-DRE + *Psav*-GFP) at zero (white column) and 30 (grey columns) dpi. *Psav*-GFP alone, population of *Psav*-GFP inoculated alone. Each value is the mean of six replicates $\pm$ *SE* (bars). Statistical significance was calculated using Student's *t* test (*$p = 0.05$)
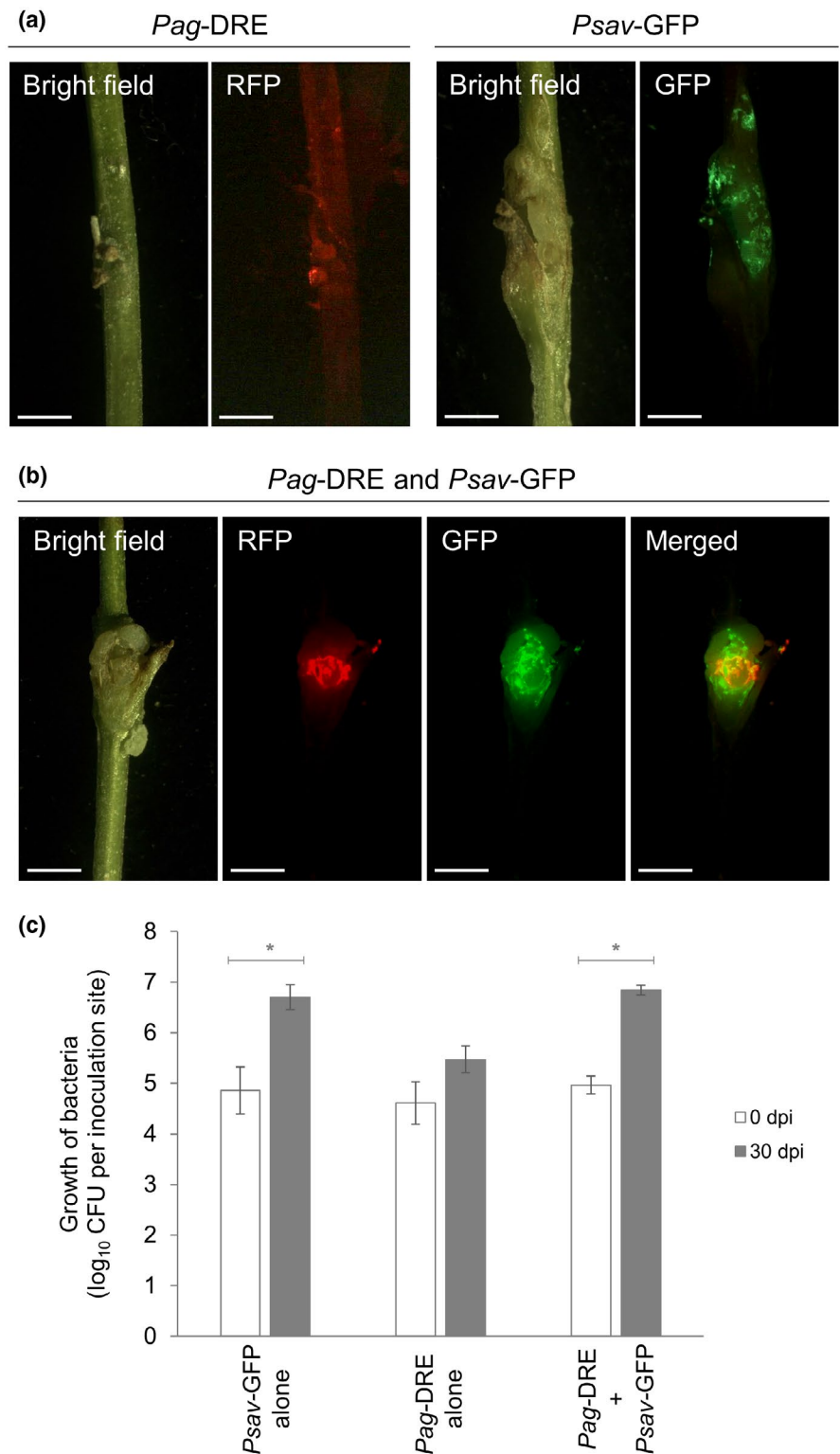
(Figure 6b). At 30 dpi, no statistically significant differences were observed between the in planta growth of *Psav*-GFP alone or in combination with *Pag*-DRE, while the growth of *Pag*-DRE was significantly stimulated in the presence of *Psav*-GFP (Figure 6c).

To better analyse the localization and distribution of the pathogen and the endophyte in knots induced by coinoculation of *Psav*-GFP and *Pag*-DRE, transversal sections were made and analysed by CLSM. The inner localization of bacteria in olive knot sections confirmed the same distribution observed by epifluorescence microscopy. While *Psav*-GFP cells were homogeneously distributed within the knot tissues, *Pag*-DRE was predominantly found forming microcolonies surrounded by *Psav*-GFP cells (Figure 7a). However, only small spots of mixed cells were found at the edges of the *Pag*-DRE microcolonies (Figure 7b).

FIGURE 7 Confocal laser scanning microscopy images of transversal sections of olive knots induced by coinoculation of RFP-labelled *Pantoea agglomerans* DAPP-PG 734 (*Pag*-DRE) and GFP-labelled *Pseudomonas savastanoi* pv. *savastanoi* DAPP-PG 722 (*Psav*-GFP) at 28 days postinoculation (a). (b) Detail of the squared region marked in (a). (c) Graphic representation of the RFP and GFP fluorescence intensities emitted along the area marked with a white line. The arrows indicate a spot where both fluorescence signals overlap. Bars = 25 μm

3 | DISCUSSION

In this study, we confirmed that *P. agglomerans* DAPP-PG 734 forms a stable interspecies community with *P. savastanoi* pv. *savastanoi* DAPP-PG 722 that allows both organisms to proliferate in olive knots, albeit in distinct microniches. Our results showed that a functional *Hrp*-1 T3SS of *P. agglomerans* DAPP-PG 734 is required for full virulence of *P. savastanoi* pv. *savastanoi* DAPP-PG 722 knots when both strains are colonizing olive knots. The fact that the coinoculation of *P. agglomerans* Pag∆*hrpY* mutant with *P. savastanoi* pv. *savastanoi* DAPP-PG 722 provoked a significant reduction in the knot volume suggests that effectors delivered by the *Hrp*-1 T3SS of *P. agglomerans* DAPP-PG 734 in olive cells suppress host defences, that is, pathogen-associated molecular pattern (PAMP)-triggered immunity (PTI) and/or effector-triggered immunity (ETI), and therefore *P. agglomerans* synergistically interacts with *P. savastanoi* pv. *savastanoi* DAPP-PG 722 inside the olive knot. However, the reduction of knot volume observed was not related to a reduction of the bacterial population size in host plant tissue. The knot volume reduction could also be caused by the lowered production of IAA by the mutants (Figure S1). In *P. agglomerans* pv. *gypsophilae* 824-1, it has been observed that T3SS effectors encoded by the Hrp regulon induce plant-derived IAA, which is essential for virulence, demonstrating a

crosstalk between the regulation of IAA and the T3SS (Chalupowicz et al., 2009, 2013; Panijel et al., 2013).

We also found that *P. agglomerans* DAPP-PG 734 encodes several effectors in its *Hrp*-1 T3SS cluster. The genes *dspA/E* and *dspF* encode for orthologs of *E. amylovora* effector DspA/E and its chaperone DspB/F (Boureau et al., 2006; Gaudriault et al., 2002). In *E. amylovora*, the DspA/E effector has a pivotal role in disease development. Mutants for this effector are unable to cause disease and to proliferate in host plants (Barny et al., 1990; Gaudriault et al., 2002) and in nonhost tobacco plants (Oh et al., 2007). The DspA/E effector belongs to the AvrE effector superfamily (PFAM protein family PF11725), which is found in many plant-pathogenic bacteria such as *P. stewartii* subsp. *stewartii*, *P. agglomerans* pv. *gypsophilae*, *Pectobacterium atroseptica*, and *P. syringae* pv. *tomato*.

Based on comparative genomics, the variable presence of T3SSs in *P. agglomerans* and related species (Figure 1), which is not related to the phylogeny of the strains, and its deviating clustering based on HrcC-HrcN-HrcU-HrcV sequences (Figure 3), confirm again that these systems are of foreign origin and can often be exchanged between species through horizontal gene transfer (Kirzinger et al., 2015). The *Hrp*-1 T3SSs including their effectors are located on (putative) plasmids (this study, Barash & Manulis-Sasson, 2009). Unfortunately, the fragmented state of the available draft genomes

containing the *Hrp*-1 T3SSs does not allow conclusions on the full backbone of the plasmids, making a direct comparison impossible. For a more detailed analysis the assembly should be improved by using long-read sequencing technologies (Dia et al., 2020; Smits, 2019).

The *Hrp*-1 T3SSs identified in this study can be separated into two groups (Figures 2 and 3). The first group includes *P. agglomerans* DAPP-PG 734 and is highly similar to the T3SSs in *P. stewartii* subsp. *stewartii* DC283 (Frederick et al., 2001) and *E. amylovora* CFBP 1430 (Oh et al., 2005; Smits et al., 2010), and has a complete HEE region. On the other hand, the second group shows deletions within the HEE region that may inactivate this region, but the genome contains additional effectors (Table 1) (Nissan et al., 2018). It thus shows that there is divergent evolution in the development of virulence to different plant hosts in these species.

In contrast to *E. toletana* DAPP-PG 735, which required the vicinity of *P. savastanoi* pv. *savastanoi* DAPP-PG 722 for its persistence and growth in olive plants (Buonaurio et al., 2015; Passos da Silva et al., 2014), we demonstrated that *P. agglomerans* DAPP-PG 734 does not localize in proximity to *P. savastanoi* pv. *savastanoi* (Figures 6 and 7). This dissimilar behaviour can be explained by invoking the QS communication system mediated by AHLs. The same AHLs (C6-3oxo- and C8-3oxo-HSL) produced by *P. savastanoi* pv. *savastanoi* DAPP-PG 722 and *E. toletana* DAPP-PG 735, which they mutually use as signal compounds, justify the proximity of the two bacterial species in the olive knots (Hosni et al., 2011). This proximity does not occur with *P. agglomerans* DAPP-PG 734, as it produces others AHLs (C4- and C6-HSL) (Hosni et al., 2011).

As reported by Hosni et al. (2011), our study confirmed that in olive plants, growth of *P. agglomerans* DAPP-PG 734 was significantly stimulated by the presence of *P. savastanoi* pv. *savastanoi* DAPP-PG 722 compared to single infections. These results indicate that both *P. agglomerans* DAPP-PG 734 and *E. toletana* DAPP-PG 735 (Hosni et al., 2011) can profit from the presence of an actively growing population of *P. savastanoi* pv. *savastanoi* DAPP-PG 722. This synergistic effect could be based on nutrient availability because the pathogen causes new plant tissue development, on metabolic sharing/complementarity, and on signal communication sharing. Similar commensal behaviour has been observed during biofilm formation by *Acinetobacter* sp. and *Pseudomonas putida* (Hansen et al., 2006). When these two species are grown in a substrate with benzyl alcohol as the sole carbon source, the growth of *P. putida* is dependent on the presence of *Acinetobacter* sp., which catabolizes the carbon source into benzoate that can be used by *P. putida* (Hansen et al., 2006). It is of note that the cells of these two species are spatially separated but with one surrounding the other, as observed for *P. savastanoi* pv. *savastanoi* DAPP-PG 722 and *P. agglomerans* DAPP-PG 734 in the olive knot (Figure 7).

In conclusion, because in other niches/systems horizontal gene transfer has been demonstrated in *Pantoea* spp. (Kirzinger et al., 2015; Manulis & Barash, 2003), it might very well be possible that *P. agglomerans* DAPP-PG 734 obtained the *Hrp*-1 T3SS and effector genes by horizontal gene transfer from pathogenic species. The presence of an active *Hrp*-1 T3SS in *P. agglomerans* DAPP-PG 734 can mitigate host defences, therefore indirectly enhancing the virulence of *P. savastanoi* pv. *savastanoi* DAPP-PG 722 in olive knots. This will have an effect on research on pathogens, as it indicates that synergistic communities can cause more harm to the host plant than a single pathogenic organism alone. Future research should also be performed to understand the role of endophytes in disease formation and also in other plant–pathogen interactions.

4 | EXPERIMENTAL PROCEDURES

4.1 | Bacterial strains, plasmids, and growth conditions

The bacterial strains and plasmids used in this study are listed in Table 2. *P. agglomerans* and *P. savastanoi* pv. *savastanoi* strains were grown at 27 °C on the following media: lysogeny broth (LB; Bertani, 1951), King's B (KB; King et al., 1954), nutrient agar (NA), or super optimal broth (SOB; Hanahan, 1983). *E. coli* was grown at 37 °C in LB broth. Antibiotics were added when required at the following final concentrations: kanamycin (Km) 100 μg/ml, gentamycin (Gm) 10 μg/ml, ampicillin (Amp) 100 μg/ml, and streptomycin (Sm) 100 μg/ml.

4.2 | Phylogenomic analyses of *P. agglomerans* and related *Pantoea* spp. based on complete genome sequences

Genome sequences of 114 *Pantoea* spp. were retrieved from the NCBI RefSeq database. Sequences were selected based on phylogeny and a maximum of 200 contigs per genome. All genome sequences were added to an EDGAR v. 2.3 database (Blom et al., 2016) for comparative genomics analysis. Five *P. agglomerans* genome sequences, which are still unpublished, were also used for this analysis. For confirmation of species, average nucleotide identity (ANI) based on BLAST analysis (Goris et al., 2007) was used with the standard settings as implemented in EDGAR. The species cut-off was set at 95%–96%. The phylogenetic tree was constructed based on concatenated alignments of each of the core genes, which was used as input for the FastTree software (Price et al., 2010) to generate approximately maximum-likelihood phylogenetic trees. Local support values are computed by FastTree using the Shimodaira-Hasegawa test and are only shown for the major nodes.

Plasmid circularity was tested by mapping the Illumina paired-end reads (Moretti et al., 2014) against the assembly using Lasergene NGen and visualized in SeqMan (DNASTAR). Read pairs that span the gap between the left and right ends indicate circularity (Smits, 2019).

Additionally, the protein sequences of the conserved proteins HrcC, HrcN, HrcU, and HrcV were extracted from the genomes using BLASTP searches (Altschul et al., 1990) and used to analyse the phylogenetic relationship between the *Hrp* T3SS of the *Pantoea* strains

studied here with T3SS of close relatives, obtained by BLASTP searches. Sequences were aligned and trees inferred using the neighbour-joining method (Saitou & Nei, 1987) conducted in MEGA 7 (Kumar et al., 2016). The percentages of replicate trees in which the associated taxa clustered together in the bootstrap test (1,000 replicates) are shown next to the branches (Felsenstein, 1985). All positions containing gaps and missing data were eliminated. There were a total of 2,128 positions in the final data set.

4.3 | Analysis of the T3SS clusters and effectors

A pan-genome analysis of all strains was performed in EDGAR to search for gene clusters encoding the T3SS (Blom et al., 2016). These gene clusters were subsequently extracted from the genome sequences, compared and visualized using different subroutines of the Lasergene v. 12.1 package (DNASTAR). Gaps in the annotation of T3SS coding sequences (CDS) were checked using BLASTX to identify the correct CDS. T3SS effectors that were not directly connected to the T3SS clusters were identified using BLASTP searches (Altschul et al., 1990) against the nr database with the restriction of the organisms to "Pantoea (taxid:5,335)". Standard settings were used for these searches.

4.4 | Recombinant DNA techniques

Recombinant DNA techniques, including digestion with restriction enzymes, agarose gel electrophoresis, purification of DNA fragments, ligation with T4 ligase, end filling with the Klenow enzyme, and transformation of *E. coli* were performed as described by Green and Sambrook (2012). Plasmids were purified using the GenElute Plasmid Miniprep Kit (Sigma-Aldrich). Triparental matings between *E. coli* and *P. agglomerans* DAPP-PG 734 were carried out using the helper strain *E. coli* HB101 carrying plasmid pRK2013 (Figurski & Helinski, 1979). DNA sequencing was performed by Macrogen Europe.

4.5 | Construction of *P. agglomerans* DAPP-PG 734 *hrpJ*, *hrpN*, and *hrpY* knockout mutants

Genomic null mutants of the *hrpJ*, *hrpN*, and *hrpY* genes (referred to as *Pag∆hrpJ*, *Pag∆hrpN*, and *Pag∆hrpY*, respectively) were created as follows. Internal fragments of *hrpJ* (326 bp), *hrpN* (434 bp), and *hrpY* (302 bp) were amplified using their respective primers, indicated in Table 2. The amplified PCR products were cloned in plasmid pKNOCK-Km (Alexeyev, 1999), generating pKNOCK-hrpJ, pKNOCK-hrpN, and pKNOCK-hrpY (Table 2). After transformation of these suicide delivery plasmids in *P. agglomerans* DAPP-PG 734, its corresponding knockout mutants were generated by homologous recombination (Alexeyev, 1999) and selected on LB-Km plates. Disruption of the *hrpJ*, *hrpN*, and *hrpY* genes was verified by PCR

using primers specific to the pKNOCK-Km vector and the genomic DNA sequences upstream and downstream of the targeted genes. The amplicons were sequenced at Macrogen Europe.

4.6 | Induction of the HR by *P. agglomerans* strains

Nicotiana tabacum 'Havana 425' plants were used for the HR assays. To prepare the inoculum, *P. agglomerans* DAPP-PG 734 and its T3SS mutants were pregrown on NA medium at 27 °C for 24 hr, and bacterial suspensions were prepared in sterile deionized water and spectrophotometrically adjusted to 10^8 cfu/ml ($OD_{600} = 0.5$). About 10 µl of bacterial suspensions or water (control) was infiltrated into the mesophyll of tobacco leaves of two different plants by using a 1-ml needleless syringe. The appearance of the HR was scored at 24 hr postinoculation (hpi).

4.7 | Plasmid complementation of the *Pag∆hrpY* mutant

Complementation of the *Pag∆hrpY* mutant with a plasmid encoding the *hrpY* gene was performed by cloning the complete sequence of the *hrpY* open reading frame (ORF) and its ribosome binding site using genomic DNA of *P. agglomerans* DAPP-PG 734, the primers hrpY_compl 1 and hrpY_compl 2 (Table 2), and Q5 High-Fidelity DNA polymerase (New England Biolabs). The amplified fragment was purified from an agarose gel using an EuroGOLD Gel Extraction Kit (EuroClone) following the manufacturer's instructions. After A-tailing (Promega), the fragment was cloned in the pGEM-T Easy vector (Promega) and confirmed by DNA sequencing (Macrogen Europe). The *hrpY* ORF was then excised from pGEM-T Easy using *Xho*I and *Spe*I and cloned in the corresponding restriction sites of plasmid pBBR-MCS-5. The resulting plasmid (pBBR-MCS-5-*hrpY*; Table 2) was purified using the GenElute Plasmid Miniprep Kit (Sigma-Aldrich) and transformed into *Pag∆hrpY* by electroporation, generating the *Pag∆hrpY* (pBBR::*hrpY*) (Table 2).

4.8 | Coinoculation assays of *P. savastanoi* pv. *savastanoi* and *P. agglomerans* in olive plants

To evaluate the effect of coinoculation, 1-year-old olive plants (cv. Frantoio) were inoculated with *P. savastanoi* pv. *savastanoi* DAPP-PG 722, *P. agglomerans* DAPP-PG 734, or its T3SS mutants alone or in combination with *P. savastanoi* pv. *savastanoi*, as described earlier (Hosni et al., 2011; Moretti et al., 2008). Bacterial growth of *P. savastanoi* pv. *savastanoi* and *P. agglomerans* strains was assessed at 0, 7, 14, 21, and 60 dpi while disease severity was evaluated 60 dpi. Two independent experiments, the first in spring (April–June; Figure 5a) and the second in autumn (September–November; Figure 5b), were carried out. The season in which the inoculation is carried out greatly affects the severity of symptoms (authors' unpublished observation).

TABLE 2 Bacterial strains isolated from the olive knots, plasmids, and primers used in this study

Strains		Relevant characteristics[a]	References
Pantoea agglomerans			
DAPP-PG 734 (wild type)		Olive knot (Italy)	Hosni et al. (2011)
Pag∆hrpJ	DAPP-PG 768	*hrpJ*::Nitrof—Km mutant of DAPP-PG 734	This study
Pag∆hrpN	DAPP-PG 769	*hrpN*::Nitrof—Km mutant of DAPP-PG 734	This study
Pag∆hrpY	DAPP-PG 770	*hrpY*::Nitrof—Km mutant of DAPP-PG 734	This study
Pag∆hrpY (pBBR::*hrpY*) DAPP-PG 778	DAPP-PG 770 (pBBRMCS5-*hrpY*)		This study
Pag-DRE		DAPP-PG 734 (pBBR2-DsRedExpress)	This study
Pseudomonas savastanoi pv. savastanoi			
DAPP-PG 722	Olive knot (Italy)		Hosni et al. (2011)
Psav-GFP		DAPP-PG 722 (pLRM1:GFP)	This study
Escherichia coli			
DH5α		F⁻, ϕ80d*lacZM15* (*lacZYA-argF*) U169, *deoR*, *recA1*, *endA*, *hsdR17* (rk ⁻ mk ⁻), *phoA*, *supE44*, *thi-1*, *gyrA96*, *relA1*	Hanahan (1983)
HB101		F⁻, rk⁻, mk⁻, leu⁻, pro⁻, thia⁻, lacZ⁻, recA⁻, endo 1⁻, Sm^R	Figurski and Helinski (1979)
Plasmids			
pKNOCK-Km	Conjugative suicide vector; Km^R		
pKNOCK-*hrpJ*	Internal *Eco*RI *hrpJ* fragment cloned in pKNOCK-Km		Alexeyev (1999)
pKNOCK-*hrpY*	Internal *Eco*RI *hrpY* fragment cloned in pKNOCK-Km		This study
pKNOCK-*hrpN*	Internal *Eco*RI *hrpN* fragment cloned in pKNOCK-Km		This study
pBBRMCS5	Broad-host-range cloning vector; Gm^R		Kovach et al. (1995)
pBBRMCS5-*hrpY*	pBBRMCS5 with 0.642-kb *Xho*I-*Spe*I fragment containing the DAPP-PG 734 *hrpY* gene		This study
pBBR2-DsRedExpress	pBBRMCS2::miniTn7PA1/04/03-DsRedExpress-a Km^R, Sm^R		Passos da Silva et al. (2014)
pLRM1-GFP	pBBRMCS5::PA1/04/03-RBSII-GFPmut3*-T0-T1, Gm^R		Rodríguez-Moreno et al. (2009)
pGEM-T Easy	Cloning vector; Amp^R		Promega
pRK2013		Mobilization helper plasmid	Figurski and Helinski (1979)
Primers			
hrpJ For	5′-GGAGAAAGGGGCTGAAGTCT-3′		This study
hrpJ Rev	5′-AACATGTTGCTGGCGGTTAG-3′		This study
hrpN For	5′-GCATGTTTGGCGATCAGGAT-3′		This study
hrpN Rev	5′-CCGAATTTGCGCTCTTCTGA-3′		This study
hrpY For	5′-CGGGTAATGGTGCTCAGGTA-3′		This study
hrpY Rev	5′-TATCTGCTCGGCCAGAACAT-3′		This study
hrpY compl 1	5′-CTCGAGAGGAGGATGGATAATA ATATTCGCCTG-3′		This study
hrpY compl 2	5′-CCTAGGGATAGCATATTTCACTA TGTCAGCATTGG-3′		This study

[a]Nitrof, nitrofurantoin; Km, kanamycin; Gm, gentamycin; Amp, ampicillin; Sm, streptomycin.

To prepare the inoculum, bacteria were grown in NA plates at 27 °C for 48 hr, suspended in sterile deionized water, and adjusted spectrophotometrically to approximately 2×10^8 cfu/ml. For bacteria inoculated alone, cell concentrations were adjusted to 10^8 cfu/ml, while for coinoculation, the two bacterial suspensions were mixed (ratio of 1:1) to obtain a final concentration of 10^8 cfu/ml for each species. Twenty microlitres of bacterial suspensions or water (control plant) were placed in wounds (four per plant) made in the bark of olive plants with a sterile scalpel (Moretti et al., 2008). Plant wounds were protected with Parafilm M until the developing knots detached it (14–21 days). Plants were maintained in transparent polycarbonate boxes to reach a relative humidity (RH) value of 90%–100% and kept in a growth chamber at 22–24 °C with illumination at 70 μmol·m^{-2}·s^{-1} with a 12-hr photoperiod. For disease severity evaluation, the knot volumes were calculated by measuring the length, width, and thickness of the knot with a Vernier caliper (Moretti et al., 2008). For bacterial growth determination, plant tissues in correspondence of the inoculated sites were cut to the wood with a sterile scalpel and homogenized in 10 mM MgCl$_2$, reaching a final volume of 1 ml at 0, 7, 14, and 21 dpi, and of 15 ml at 60 dpi. One hundred microlitres of serially diluted homogenates was spread on NA plates and the colonies formed at 27 °C were counted after 24 and 48 hr.

4.9 | Localization of *P. agglomerans* and *P. savastanoi* pv. *savastanoi* within the knot

The distribution of *P. agglomerans* DAPP-PG 734 and *P. savastanoi* pv. *savastanoi* DAPP-PG 722 within knots was assessed by epifluorescence stereoscopic microscopy as well as CLSM using the fluorescently labelled strains *Psav*-GFP and *Pag*-DRE (Table 2). To obtain green fluorescent protein (GFP) and DsRedExpress (DRE) transformants, plasmids pLRM1-GFP (Rodríguez-Moreno et al., 2009) and pBBR2-DsRedExpress (Passos da Silva et al., 2014) were transferred to *P. savastanoi* pv. *savastanoi* DAPP-PG 722 and *P. agglomerans* DAPP-PG 734, respectively, by triparental mating using *E. coli* DH5α (Table 2).

For the inoculation of *Psav*-GFP and *Pag*-DRE, in vitro micropropagated olive plants derived from a cv. Arbequina seed were used. Olive plants were micropropagated and rooted (Rodriguez-Moreno et al., 2008) in Driver Kuniyuki walnut (DKW) medium (Driver & Kuniyuki, 1984). Rooted explants were transferred to DKW medium without hormones and kept for at least 2 weeks in a growth chamber at 25 °C with a 16-hr photoperiod and a light intensity of 35 μmol·m^{-2}·s^{-1} prior to infection. The in vitro olive plants were 60–80 mm long (1–2 mm stem diameter) and contained three to five internodal fragments. Micropropagated olive plants were wounded by excision of an intermediate leaf and infected in the stem wound with a bacterial suspension under sterile conditions. For inoculum preparation, bacteria were grown in LB-Gm or LB-Km plates at 27 °C for 48 hr, resuspended in 10 mM MgCl$_2$ and adjusted spectrophotometrically to approximately 10^7 cfu/ml. For

coinoculation, the two bacterial suspensions were mixed (ratio 1:1) to obtain a final concentration of 10^7 cfu/ml of each species. Two microlitres of the bacterial suspension or water (for control plants) were placed in the wounds (two per plant) and the plants were incubated in a growth chamber at 25 °C as described above. The bacterial population size was evaluated at 0 and 30 dpi according to Rodríguez-Moreno et al. (2008).

To visualize the bacterial infections of the knots in real time, whole knots were examined at 28 dpi using a fluorescence stereomicroscope (Leica MZ FLIII) equipped with a 100 W mercury lamp, a GFP2 filter (excitation, 480/40 nm; emission 510LP), and a red fluorescent protein (RFP) filter (excitation, 546/10 nm; emission, 570LP). Images were captured using a high-resolution digital camera (Nikon; DXM 1200). To visualize bacterial infection within the knots by CLSM, knots were sampled at 1 cm above and below the inoculation point at 30 dpi. Transversal sections were examined by using an inverted CLSM (model SP5 II; Leica) equipped with detectors and filters that simultaneously allow detection of green and red fluorescence. Images of green fluorescence were acquired with an excitation wavelength of 488 nm and an emission BP filter for 500–550 nm; red fluorescence emission was recorded in the interval between 575 and 625 nm. The images were acquired by sequential scan analysis using Leica LAS AF software (Passos da Silva et al., 2014) and processed with ImageJ (Schneider et al., 2012).

4.10 | Statistical analysis

All experiments were independently repeated two to four times (see the figure legends for further details).

Disease severity data were analysed by fitting an analysis of variance (ANOVA) model, where the strain was included as an explanatory factor. Means were compared by using a Duncan's multiple range test.

Data from bacterial growth in planta were transformed into base 10 logarithms (to correct for heteroscedasticity) and were used to parameterize a linear mixed model (Garrett et al., 2004; Onofri et al., 2010) describing the relationship between the number of bacterial cells and the square root of time (for each strain/group) by way of second-order polynomial function. Plant and inoculation position within the plant were added as random effects to the model to account for grouped data. The model parameters were estimated using the maximum-likelihood approach as implemented in the 'nlme' package in the R statistical environment (Venables & Ripley, 2002). The differences among strains/groups in terms of growth kinetics were assessed by using likelihood ratio tests. For each bacterial strain, the relationship between the number of cells (log$_{10}$ transformed) and the hours postinoculation was investigated by means of a second-order polynomial model. The likelihood ratio test was used to assess the differences between wildtype and mutant strains under the R statistical environment (R Core Team, 2020).

CONFLICT OF INTEREST

The authors have declared that no conflict of interest exists.

DATA AVAILABILITY STATEMENT

The data that support the findings of this study are available from the corresponding author upon reasonable request.

ORCID

Chiaraluce Moretti https://orcid.org/0000-0003-1500-7320
Cayo Ramos https://orcid.org/0000-0002-2362-5041

REFERENCES

Alexeyev, M.F. (1999) The pKNOCK series of broad-host-range mobilizable suicide vectors for gene knockout and targeted DNA insertion into the chromosome of gram-negative bacteria. *BioTechniques*, 26, 824–828.

Altschul, S.F., Gish, W., Miller, W., Myers, E.W. & Lipman, D.J. (1990) Basic local alignment search tool. *Journal of Molecular Biology*, 215, 403–410.

Barash, I. & Manulis-Sasson, S. (2009) Recent evolution of bacterial pathogens: the gall-forming *Pantoea agglomerans* case. *Annual Review of Phytopathology*, 47, 133–152.

Barny, M.A., Guinebretiere, M., Marcais, B., Coissac, E., Paulin, J. & Laurent, J. (1990) Cloning of a large gene cluster involved in *Erwinia amylovora* CFBP1430 virulence. *Molecular Microbiology*, 4, 777–786.

Bertani, G. (1951) Studies on lysogenesis I: the mode of phage liberation by lysogenic *Escherichia coli*. *Journal of Bacteriology*, 62, 293–300.

Blom, J., Kreis, J., Spänig, S., Juhre, T., Bertelli, C., Ernst, C. et al. (2016) EDGAR 2.0: an enhanced software platform for comparative gene content analyses. *Nucleic Acids Research*, 44, W22–W28.

Boureau, T., El Maarouf-Bouteau, H., Garnier, A., Brisset, M.-N., Perino, C., Pucheu, I. et al. (2006) DspA/E, a type III effector essential for *Erwinia amylovora* pathogenicity and growth *in planta*, induces cell death in host apple and nonhost tobacco plants. *Molecular Plant-Microbe Interactions*, 19, 16–24.

Buonaurio, R., Moretti, C., Da Silva, D.P., Cortese, C., Ramos, C. & Venturi, V. (2015) The olive knot disease as a model to study the role of interspecies bacterial communities in plant disease. *Frontiers in Plant Science*, 6, 434.

Caballo-Ponce, E., Meng, X., Uzelac, G., Halliday, N., Cámara, M., Licastro, D., et al. (2018) Quorum sensing in *Pseudomonas savastanoi* pv. *savastanoi* and *Erwinia toletana*: Role in virulence and interspecies interactions in the olive knot. *Applied and Environmental Microbiology*, 84, e00950-18.

Caballo-Ponce, E., Murillo, J., Martínez-Gil, M., Moreno-Pérez, A., Pintado, A. & Ramos, C. (2017a) Knots untie: Molecular determinants involved in knot formation induced by *Pseudomonas savastanoi* in woody hosts. *Frontiers in Plant Science*, 8, 1089.

Caballo-Ponce, E., van Dillewijn, P., Wittich, R.M. & Ramos, C. (2017b) WHOP, a genomic region associated with woody hosts in the *Pseudomonas syringae* complex contributes to the virulence and fitness of *Pseudomonas savastanoi* pv. *savastanoi* in olive plants. *Molecular Plant-Microbe Interactions*, 30, 113–126.

Chalupowicz, L., Barash, I., Panijel, M., Sessa, G. & Manulis-Sasson, S. (2009) Regulatory interactions between quorum-sensing, auxin, cytokinin, and the Hrp regulon in relation to gall formation and epiphytic fitness of *Pantoea agglomerans* pv. *gypsophilae*. *Molecular Plant-Microbe Interactions*, 22, 849–856.

Chalupowicz, L., Manulis-Sasson, S., Itkin, M., Sacher, A., Sessa, G. & Barash, I. (2008) Quorum-sensing system affects gall development incited by *Pantoea agglomerans* pv. *gypsophilae*. *Molecular Plant-Microbe Interactions*, 21, 1094–1105.

Chalupowicz, L., Weinthal, D., Gaba, V., Sessa, G., Barash, I. & Manulis-Sasson, S. (2013) Polar auxin transport is essential for gall formation by *Pantoea agglomerans* on gypsophila. *Molecular Plant Pathology*, 14, 185–190.

Correa, V.R., Majerczak, D.R., Ammar, E.-D., Merighi, M., Pratt, R.C., Hogenhout, S.A. et al. (2012) The bacterium *Pantoea stewartii* uses two different type III secretion systems for colonizing its plant host and insect vector. *Applied and Environmental Microbiology*, 78, 6327–6336.

De Maayer, P., Chan, W.-Y., Blom, J., Venter, S.N., Duffy, B., Smits, T.H.M. et al. (2012) The large universal *Pantoea* plasmid LPP-1 plays a major role in biological and ecological diversification. *BMC Genomics*, 13, 625.

Dia, N.C., Rezzonico, F., Smits, T.H.M. & Pothier, J.F. (2020) Complete or high-quality draft genome sequences of six *Xanthomonas hortorum* species level clade strains sequenced with short- and long-read technologies. *Microbiology Resource Announcements*, 9, e00828-20.

Driver, J.A. & Kuniyuki, A.H. (1984) *In vitro* propagation of Paradox walnut rootstock [*Juglans hindsii* X *Juglans regia*, tissue culture]. *HortScience*, 18, 506–509.

Felsenstein, J. (1985) Confidence limits on phylogenies an approach using the bootstrap. *Evolution*, 39, 783–791.

Figurski, D.H. & Helinski, D.R. (1979) Replication of an origin-containing derivative of plasmid RK2 dependent on a plasmid function provided in trans. *Proceedings of the National Academy of Sciences of the United States of America*, 76, 1648–1652.

Frederick, R.D., Ahmad, M., Majerczak, D.R., Arroyo-Rodríguez, A.S., Manulis, S. & Coplin, D.L. (2001) Genetic organization of the *Pantoea stewartii* subsp. *stewartii* hrp gene cluster and sequence analysis of the *hrpA*, *hrpC*, *hrpN*, and *wtsE* operons. *Molecular Plant-Microbe Interactions*, 14, 1213–1222.

Garrett, K.A., Madden, L.V., Hughes, G. & Pfender, W.F. (2004) New applications of statistical tools in plant pathology. *Phytopathology*, 94, 999–1003.

Gaudriault, S., Paulin, J.P. & Barny, M.A. (2002) The DspB/F protein of *Erwinia amylovora* is a type III secretion chaperone ensuring efficient intrabacterial production of the Hrp-secreted DspA/E pathogenicity factor. *Molecular Plant Pathology*, 3, 313–320.

Goris, J., Konstantinidis, K.T., Klappenbach, J.A., Coenye, T., Vandamme, P. & Tiedje, J.M. (2007) DNA–DNA hybridization values and their relationship to whole-genome sequence similarities. *International Journal of Systematic and Evolutionary Microbiology*, 57, 81–91.

Green, M.R. & Sambrook, J. (2012) *Molecular cloning: a laboratory manual*, Cold Spring Harbor, NY, USA: Cold Spring Harbor Laboratory Press.

Hanahan, D. (1983) Studies on transformation of *Escherichia coli* with plasmids. *Journal of Molecular Biology*, 166, 557–580.

Hansen, S.K., Rainey, P.B., Haagensen, J.A.J. & Molin, S. (2006) Evolution of species interactions in a biofilm. *Nature*, 445, 533–536.

Hosni, T. (2010) *Interaction between* Pseudomonas savastanoi *pv.* savastanoi, *the causal agent of olive knot, and the endophytic bacterial species associated with the knot*. PhD thesis, University of Perugia.

Hosni, T., Moretti, C., Devescovi, G., Suarez-Moreno, Z.R., Fatmi, M.B., Guarnaccia, C. et al. (2011) Sharing of quorum-sensing signals and role of interspecies communities in a bacterial plant disease. *ISME Journal*, 5, 1857–1870.

Hu, Y., Huang, H., Cheng, X., Shu, X., White, A.P., Stavrinides, J. et al. (2017) A global survey of bacterial type III secretion systems and their effectors. *Environmental Microbiology*, 19, 3879–3895.

Kamber, T., Smits, T.H.M., Rezzonico, F. & Duffy, B. (2012) Genomics and current genetic understanding of *Erwinia amylovora* and the fire blight antagonist *Pantoea vagans*. *Trees*, 26, 227–238.

King, E.O., Ward, M.K. & Raney, D.E. (1954) Two simple media for the demonstration of pyocyanin and fluorescin. *Journal of Laboratory and Clinical Medicine*, 44, 301–307.

Kirzinger, M.W., Butz, C.J. & Stavrinides, J. (2015) Inheritance of *Pantoea* type III secretion systems through both vertical and horizontal transfer. *Molecular Genetics and Genomics*, 290, 2075–2088.

Kobayashi, D.Y. & Palumbo, J.D. (2000) Bacterial endophytes and their effects on plants and uses in agriculture. In: Bacon, C.W. & White, J.F. (Eds.) *Microbial endophytes*. New York: Marcel Dekker, pp. 99–233.

Kovach, M.E., Elzer, P.H., Steven Hill, D., Robertson, G.T., Farris, M.A., Roop R.M. & Peterson K.M. (1995) Four new derivatives of the broad-host-range cloning vector pBBR1MCS, carrying different antibiotic-resistance cassettes. *Gene*, 166, 175–176.

Kumar, S., Stecher, G. & Tamura, K. (2016) MEGA7: molecular evolutionary genetics analysis version 7.0 for bigger datasets. *Molecular Biology and Evolution*, 33, 1870–1874.

Lindow, S.E. & Brandl, M.T. (2003) Microbiology of the phyllosphere. *Applied and Environmental Microbiology*, 69, 1875–1883.

Manulis, S. & Barash, I. (2003) *Pantoea agglomerans* pvs. *gypsophilae* and *betae*, recently evolved pathogens? *Molecular Plant Pathology*, 4, 307–314.

Manulis, S., Gafni, Y., Clark, E., Zutra, D., Ophir, Y. & Barash, I. (1991a) Identification of a plasmid DNA probe for detection of strains of *Erwinia herbicola* pathogenic on *Gypsophila paniculata*. *Phytopathology*, 81, 54–57.

Manulis, S., Valinski, L., Gafni, Y. & Hershenhorn, J. (1991b) Indole-3-acetic acid biosynthetic pathways in *Erwinia herbicola* in relation to pathogenicity on *Gypsophila paniculata*. *Physiological and Molecular Plant Pathology*, 39, 161–171.

Merighi M., Majerczak D.R., Stover E.H. & Coplin D.L. (2003) The HrpX/HrpY two-component system activates *hrpS* expression, the first step in the regulatory cascade controlling the *Hrp* regulon in *Pantoea stewartii* subsp. *stewartii*. *Molecular Plant-Microbe Interactions*, 16, 238–248.

Merighi, M., Majerczak, D.R., Zianni, M., Tessanne, K. & Coplin, D.L. (2006) Molecular characterization of *Pantoea stewartii* subsp. *stewartii* HrpY, a conserved response regulator of the Hrp type III secretion system, and its interaction with the *hrpS* promoter. *Journal of Bacteriology*, 188, 5089–5100.

Mor, H., Manulis, S., Zuck, M., Nizan, R., Coplin, D.L. & Barash, I. (2001) Genetic organization of the *hrp* gene cluster and *dspAE/BF* operon in *Erwinia herbicola* pv. *gypsophilae*. *Molecular Plant-Microbe Interactions*, 14, 431–436.

Moreno-Pérez, A., Pintado, A., Murillo, J., Caballo-Ponce, E., Tegli, S., Moretti, C. et al. (2020) Host range determinants of *Pseudomonas savastanoi* pathovars of woody hosts revealed by comparative genomics and cross-pathogenicity tests. *Frontiers in Plant Science*, 11, 973.

Moretti, C., Cortese, C., Passos da Silva, D., Venturi, V., Torelli, E., Firrao, G. et al. (2014) Draft genome sequence of a hypersensitive reaction-inducing *Pantoea agglomerans* strain isolated from olive knots caused by *Pseudomonas savastanoi* pv. *savastanoi*. *Genome Announcements*, 2, e00774-14.

Moretti, C., Ferrante, P., Hosni, T., Valentini, F., D'Onghia, A., Fatmi, M.B. et al. (2008) Characterization of *Pseudomonas savastanoi* pv. *savastanoi* strains collected from olive trees in different countries. In: Fatmi,

M.B., Collmer, A., Iacobellis, N.S., Mansfield, J.W., Murillo, J., Schaad, N.W. & Ullrich, M. (Eds.) *Pseudomonas syringae pathovars and related pathogens – Identification, epidemiology and genomics*. Berlin: Springer Science+ Business Media, BV, pp. 321–329.

Moretti, C., Trabalza, S., Granieri, L., Caballo-Ponce, E., Devescovi, G., Del Pino, A.M. et al. (2019) A Na^+/Ca^{2+} exchanger of the olive pathogen *Pseudomonas savastanoi* pv. *savastanoi* is critical for its virulence. *Molecular Plant Pathology*, 20, 716–730.

Nissan, G., Gershovits, M., Morozov, M., Chalupowicz, L., Sessa, G., Manulis-Sasson, S. et al. (2018) Revealing the inventory of type III effectors in *Pantoea agglomerans* gall-forming pathovars using draft genome sequences and a machine-learning approach. *Molecular Plant Pathology*, 19, 381–392.

Oh, C.S., Kim, J.F. & Beer, S.V. (2005) The *Hrp* pathogenicity island of *Erwinia amylovora* and identification of three novel genes required for systemic infection. *Molecular Plant Pathology*, 6, 125–138.

Oh, C.S., Martin, G.B. & Beer, S.V. (2007) DspA/E, a type III effector of *Erwinia amylovora*, is required for early rapid growth in *Nicotiana benthamiana* and causes NbSGT1-dependent cell death. *Molecular Plant Pathology*, 8, 255–265.

Onofri, A., Carbonell, E.A., Piepho, H.P., Mortimer, A.M. & Cousens, R.D. (2010) Current statistical issues in weed research. *Weed Research*, 50, 5–24.

Panijel, M., Chalupowicz, L., Sessa, G., Manulis-Sasson, S. & Barash, I. (2013) Global regulatory networks control the *hrp* regulon of the gall-forming bacterium *Pantoea agglomerans* pv. *gypsophilae*. *Molecular Plant-Microbe Interactions*, 26, 1031–1043.

Passos da Silva, D., Castañeda-Ojeda, M.P., Moretti, C., Buonaurio, R., Ramos, C. & Venturi, V. (2014) Bacterial multispecies studies and microbiome analysis of a plant disease. *Microbiology*, 160, 556–566.

Price, M.N., Dehal, P.S. & Arkin, A.P. (2010) FastTree 2 – aproximately maximum-likelihood trees for large alignments. *PLoS One*, 5, e9490.

Quesada, J.M., Penyalver, R. & López, M.M. (2012) Epidemiology and control of plant diseases caused by phytopathogenic bacteria: the case of olive knot disease caused by *Pseudomonas savastanoi* pv. *savastanoi*. In: Cumagun, C.J. (ed.) *Plant pathology*. Rijeda, Croatia: In Tech, pp. 299–326.

R Core Team (2020) *R: A language and environment for statistical computing*. R Foundation for Statistical Computing, Vienna, Austria. Available at: https://www.r-project.org [Accessed 7 July 2021].

Ramos, C., Matas, I.M., Bardaji, L., Aragón, I.M. & Murillo, J. (2012) *Pseudomonas savastanoi* pv. *savastanoi*: some like it knot. *Molecular Plant Pathology*, 13, 998–1009.

Rodríguez-Moreno, L., Barceló-Muñoz, A. & Ramos, C. (2008) *In vitro* analysis of the interaction of *Pseudomonas savastanoi* pvs. *savastanoi* and *nerii* with micropropagated olive plants. *Phytopathology*, 98, 815–822.

Rodríguez-Moreno, L., Jiménez, A.J. & Ramos, C. (2009) Endopathogenic lifestyle of *Pseudomonas savastanoi* pv. *savastanoi* in olive knots. *Microbial Biotechnology*, 2, 476–488.

Roper, M.C. (2011) *Pantoea stewartii* subsp. *stewartii*: lessons learned from a xylem-dwelling pathogen of sweet corn. *Molecular Plant Pathology*, 12, 628–637.

Saitou, N. & Nei, M. (1987) The neighbor-joining method: a new method for reconstructing phylogenetic trees. *Molecular Biology and Evolution*, 4, 406–425.

Schneider, C.A., Rasband, W.S. & Eliceiri, K.W. (2012) NIH Image to ImageJ: 25 years of image analysis. *Nature Methods*, 9, 671–675.

Schroth, M., Osgood, J. & Miller, T. (1973) Quantitative assessment of the effect of the olive knot disease on olive yield and quality. *Phytopathology*, 63, 1064–1065.

Smits, T.H.M. (2019) The importance of genome sequence quality to microbial comparative genomics research. *BMC Genomics*, 20, 662.

Smits, T.H.M., Rezzonico, F., Kamber, T., Blom, J., Goesmann, A., Frey, J.E. et al. (2010) Complete genome sequence of the fire blight pathogen

Erwinia amylovora CFBP 1430 and comparison to other *Erwinia* spp. *Molecular Plant-Microbe Interactions*, 23, 384–393.

Smits, T.H.M., Rezzonico, F., Kamber, T., Blom, J., Goesmann, A., Ishimaru, C.A. et al. (2011) Metabolic versatility and antibacterial metabolite biosynthesis are distinguishing genomic features of the fire blight antagonist *Pantoea vagans* C9–1. *PLoS One*, 6, e22247.

Venables, W.N. & Ripley, B.D. (Eds.) (2002) Random and mixed effects. In: *Modern applied statistics with S*. New York, USA: Springer, pp. 271–300.

Walterson, A.M. & Stavrinides, J. (2015) *Pantoea*: Insights into a highly versatile and diverse genus within the *Enterobacteriaceae*. *FEMS Microbiology Reviews*, 39, 968–984.

Weinthal, D.M., Barash, I., Panijel, M., Valinsky, L., Gaba, V. & Manulis-Sasson, S. (2007) Distribution and replication of the pathogenicity plasmid pPATH in diverse populations of the gall-forming bacterium *Pantoea agglomerans*. *Applied and Environmental Microbiology*, 73, 7552–7561.

SUPPORTING INFORMATION

Additional Supporting Information may be found online in the Supporting Information section.